THE JOURNAL OF PHYSICAL CHEMISTRY C

Article

pubs.acs.org/JPCC

Nafion Induced Surface Confinement of Oxygen in Carbon-Supported Oxygen Reduction Catalysts

Jerzy Chlistunoff* and José-María Sansiñena

Los Alamos National Laboratory P.O. Box 1663, Los Alamos, New Mexico 87545, United States

ABSTRACT: Surface confinement of oxygen inside layers of Nafion self-assembled on carbon-supported oxygen reduction reaction (ORR) catalysts was studied. It is demonstrated that oxygen accumulates in the hydrophobic component of the polymer remaining in contact with the carbon surface. The amount of surface confined oxygen increases with the degree of carbon surface graphitization, which promotes the self-assembly of the polymer. Planar macrocyclic ORR catalysts possessing a delocalized system of π electrons such as Co and Fe porphyrins and phthalocyanines have virtually no effect on the surface confinement of oxygen, in accordance with their structural similarity to graphitic carbon surfaces where they adsorb. Platinum particles in carbon-supported ORR catalysts with high metal contents (20%) disrupt the self-assembly of Nafion and virtually eliminate the oxygen confinement, but the phenomenon is still observed for low Pt loading (4.8%) catalysts.

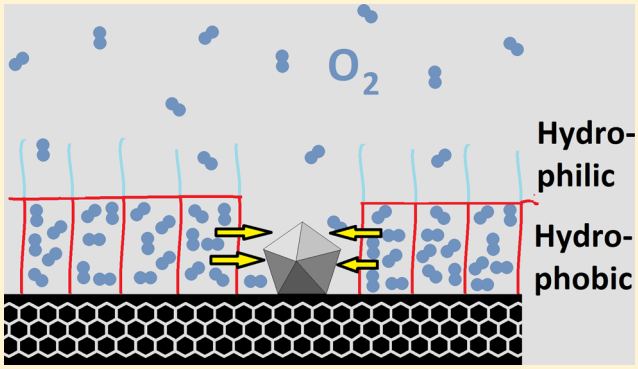

INTRODUCTION

In a recent paper, we reported the existence of oxygen adsorption on the surface of a polyaniline-based heat-treated Fe/N/C catalyst of oxygen reduction reaction (ORR) in sulfuric acid media.[1] The adsorption isotherm exhibited the Langmuirian[2] characteristics, *i.e.*, did not display any noticeable repulsive or attractive interactions between oxygen molecules in the adsorbed layer. As the amount of adsorbed oxygen correlated with the surface density of the iron sites, we postulated that the adsorption occurred either in the close proximity of or directly on the catalytically active Fe sites. On the basis of previous work,[3−5] the latter comprise iron centers coordinated by four in-plane pyridinic nitrogen atoms belonging to either a single (N_4) or two separate coplanar (N_{2+2} coordination) graphene planes and arranged like two phenanthroline molecules. In the course of our more recent studies on oxygen reduction catalysis by transition metal macrocyclic complexes, *e.g.*, porphyrins, phthalocyanines, and corroles,[6] we found the presence of similar adsorption phenomena in the presence of aqueous electrolytes. The active centers of the macrocyclic complexes are structurally similar to those postulated for the Fe/N/C composites in that they have a similar in-plane N_4 coordination of the metal centers and a π-electron rich environment surrounding them. However, an interesting fact about the oxygen adsorption observed for the macrocycles was that it occurred irrespective of whether the active center was Fe(III) or Co(II), which suggested no direct involvement of the metal center in the phenomenon. On the other hand, a direct oxygen−metal center interaction is a prerequisite for the metal center catalyzed oxygen reduction. While some reports on heat-treated ORR catalysts demonstrate that oxygen reduction may be catalyzed by the active sites containing no metal,[7,8] there is no doubt that the catalysis of oxygen reduction by macrocyclic complexes of transition metals is invariably associated with the presence of red−ox active metal centers.[9−11] The same is also true for catalytically active metals, such as platinum, where ORR involves the formation of surface oxide (hydroxide) species.[12,13] In either case, the interaction of oxygen with the active site involves at least a partial charge transfer (CT) between the entities, whereas a small free energy of oxygen adsorption on the heat-treated Fe/N/C catalysts[1] (−15.7 kJ mol^{-1}) was consistent with the lack of CT between oxygen and the catalyst surface. Intrigued by the apparent role of weak molecular interactions in the only once reported[1] and yet unexplained oxygen adsorption phenomenon, we decided to reveal the factors responsible for its appearance and determine the nature of the adsorption sites. The phenomenon is interesting from a fundamental point of view. In addition, its presence can lead to errors in the determination of the catalytic activities of ORR catalysts measured in aqueous media. The latter are nearly exclusively determined using hydrodynamic voltammetry, *i.e.*, the rotating disk electrode (RDE) or rotating ring disk electrode (RRDE) technique. At sufficiently slow scan rates, the transport of dissolved oxygen to an RDE (RRDE) is determined exclusively by the electrode rotation rate and the hydrodynamic properties of the electrolyte solution.[14] Those parameters and the actual electrode potential, but not the (slow) scan rate, determine the reduction current of dissolved oxygen. However, adsorbed oxygen will produce a nonzero reduction current independent

Received: September 20, 2016
Revised: November 13, 2016
Published: November 17, 2016

DOI: 10.1021/acs.jpcc.6b09523
J. Phys. Chem. C 2016, 120, 28038−28048

of the rotation rate (oxygen transport from solution) but proportional to the potential scan rate.[14] Such contribution to the measured current disappears only when the electrode potential is held constant, *e.g.*, in less frequently used and time-consuming staircase voltammetry[15] with long potential step duration.

The model systems employed in the current study were simple molecular ORR catalysts comprising of carbon-supported iron and cobalt phthalocyanines and porphyrins. For comparison, we also performed a series of similar experiments with three carbon-supported Pt catalysts. As opposed to the molecular catalysts, where isolated central atoms are responsible for ORR catalysis, entire crystal facets of carbon-supported Pt nanocrystals in the commercial catalysts participate in the reaction. We found that oxygen adsorption was induced by the self-assembly of Nafion on high surface area carbons used as ORR catalyst supports.[16] While the ability of Nafion to self-assemble on a variety of smooth and flat surfaces has been well-known,[17] the self-assembly of the ionomer on high surface area carbons has not been reported until very recently.[16] The links between oxygen adsorption and Nafion self-assembly on high surface area carbons as well as the nature of the adsorption process are presented and discussed in the following sections of the manuscript.

EXPERIMENTAL SECTION

The following macrocyclic complexes were obtained from Aldrich and used as received: iron(III) tetraphenylporphyrin chloride ((5,10,15,20-tetraphenyl-21*H*,23*H*-porphine)iron(III) chloride, > 94%, hereafter called FeTPPCl), iron(III) phthalocyanine chloride (~95%, hereafter called FePCCl), iron(III) octaethylporphyrin chloride ((2,3,7,8,12,13,17,18-octaethyl-21*H*,23*H*-porphine)iron(III) chloride, hereafter called FeOEPCl), cobalt(II) phthalocyanine (97%, hereafter called CoPC), cobalt(II) tetramethoxyphenylporphyrin ((5,10,15,20-tetrakis(4-methoxyphenyl)-21*H*,23*H*-porphine)-cobalt(II), 97%, hereafter called CoTMeOPP), cobalt(II) octaethylporphyrin ((2,3,7,8,12,13,17,18-octaethyl-21*H*,23*H*-porphine)cobalt(II), hereafter called CoOEP), cobalt(II) tetraphenylporphyrin ((5,10,15,20-tetraphenyl-21*H*,23*H*-porphine)cobalt(II), 85%, hereafter called CoTPP).

Anhydrous dichloromethane (DCM, ≥ 99.8% with 50−150 ppm amylene as stabilizer, Sigma-Aldrich) and Vulcan XC72, a high surface area (205−250 $m^2\ g^{-1}$)[18−21] carbon with the average particle size between 30 and 40 nm[22,23] (Cabot) were used as received.

All experiments were performed using 0.5 mol dm^{-3} H_2SO_4 at 25 °C as the background electrolyte. The electrolyte was prepared using a commercial sulfuric acid (Certified ACS Plus, Fisher Chemical) and Millipore water.

The working electrode in RRDE and numerous voltammetric experiments was a Pine model AFE7R9GCPT electrode with a glassy carbon disk and a platinum ring. During RRDE experiments, the ring potential was held at +1.2 V, where all H_2O_2 formed in ORR could be oxidized at the transport controlled rate, which enabled the determination of the number of electrons (n) transferred in ORR using the following equation: $n = 4I_D/(I_D + I_R/N)$, where I_D and I_R stand for the disk and ring currents, respectively. The nominal collection efficiency (N) of the RRDE (37%) was confirmed by independent measurements using potassium ferricyanide in potassium chloride electrolyte solutions. In some voltammetric experiments a 3 mm glassy carbon disk (Bioanalytical Systems), a 1.6 mm Pt disk (Bioanalytical Systems) and homemade 4.8 mm highly oriented pyrolytic graphite (HOPG) disk electrodes were used. The latter were fabricated by masking a 7 mm × 7 mm × 1 mm HOPG platelet from SPI Supplies (grade SPI-2, mosaic angle 0.8° ± 0.2°, lateral grain size up to 0.5−1 mm) with polyimide Kapton tape using the methodology described previously.[16]

The deposition of Pt nanoparticles on HOPG was performed using a technique similar to that applied by Ju and co-workers for palladium.[24] A freshly prepared HOPG disk electrode was placed under potential (0.84 V vs RHE) in a 2 mM H_2PtCl_6 solution in 0.5 M H_2SO_4. The potential was applied in order to prevent a spontaneous Pt deposition. After 10 s, a 100 ms potential pulse to 5 V was applied to create oxidized surface sites for Pt deposition. Ten seconds after the first pulse, a 20 ms potential pulse (−0.06 V vs RHE) was applied to initiate fast H_2PtCl_6 reduction, guaranteeing instantaneous Pt nucleation. After the pulse, the potential was changed to 0.24 V vs RHE in order to deposit Pt on the nuclei deposited at −0.06 V. The electrode was held at 0.24 V vs RHE for 20 s after which the potential was changed again to 0.84 V to stop the growth of Pt particles. The electrode was removed under potential from the solution, rinsed with Millipore water and dried in air. The electrochemically active surface area of such deposited Pt (typically ~2.4×10^{-2} cm^2) was determined from cyclic voltammetry in deoxygenated sulfuric acid solution and corresponded to ~13% of the surface area of the HOPG disk. Neither the size nor the surface distribution of the particles was determined.

The counter electrode in all experiments was a graphite rod, whereas the reference electrode was a hydrogen electrode utilizing 6% H_2 in Ar in equilibrium with a Pt black coated platinum wire immersed in 0.5 mol dm^{-3} H_2SO_4. The equilibrium potential of the reference electrode at Los Alamos elevation (2100 m above sea level) is 39 mV more positive than the potential of a reversible hydrogen electrode (RHE) in the respective solution at the sea level.[1]

Oxygen concentration in the studied solutions was adjusted by using either pure oxygen or its mixtures with argon as the purging gas. The actual oxygen concentration in solution was determined from the corresponding limiting RRDE currents corrected for the number of electrons transferred in ORR and the respective corrected currents measured for oxygen saturated solution (8.65×10^{-4} mol dm^{-3} at Los Alamos elevation of 2100 m[1]).

Two well-characterized[18,22,25−27] Pt catalysts supported on Vulcan were used in the study: 20% Pt (BASF) and 4.8% Pt (TEC10V05E, Tanaka Kikinzoku Kogyo). The third studied Pt (4.8%) catalyst was supported on graphitized carbon. Its properties were not disclosed by the manufacturer. The X-ray diffraction and BET measurements were performed by the authors of the paper. In similarity to Vulcan, the carbon support in that catalyst exhibited low porosity (<2 nm), but the BET surface area of the catalyst (157 $m^2\ g^{-1}$) was significantly lower than that of Vulcan, whereas the Pt particle size (4.8 nm from Scherrer equation[28]) larger than that (2.1−2.6 nm) for the remaining Pt catalysts.[18,25−27] As in our previous paper,[16] the three Pt catalysts will be hereafter called Pt20V (20% BASF), Pt4.8V (4.8% Tanaka), and Pt4.8G (Pt on graphitized support), respectively.

The catalyst inks for macrocyclic ORR catalysts were prepared using the procedure described in our previous paper.[16] Briefly, ~ 40 mg of Vulcan XC72 were mixed with a

DOI: 10.1021/acs.jpcc.6b09523
J. Phys. Chem. C 2016, 120, 28038−28048

few milligrams of the desired macrocycle and 2−4 cm^3 of dichloromethane and slowly sonicated to dryness. The residue was sonicated for around 1 h with 8 cm^3 of isopropanol (IPA) and small quantities of 5% Nafion solution (Ion Power, Inc.). The inks of Pt catalysts were prepared by mixing the solids with IPA and Nafion followed by sonication. The amount of 5% Nafion solution in the catalyst inks will be denoted[16] by R and corresponds to the ratio of volume of the 5% Nafion solution expressed in microliters to the mass of the carbon support expressed in milligrams. The value of R varied from 0 to 2.7 μL per 1 mg of the carbon support, *i.e.*, $R = 1$ corresponds to 1 μL of the Nafion solution used for 1 mg of the carbon support and is equivalent to 46.8 μg of pure Nafion per 1 mg of the support. All inks were stored in tightly closed glass vials at room temperature.

A Pine Instruments bipotentiostat model AFCBP1 controlled by Aftermath software (Pine Instruments) was used in all experiments. As in our previous study,[16] devoted to the self-assembly of Nafion on high surface area carbons, the experiments were performed for a constant total loading of 0.1 mg of the carbon support, which corresponded to ∼0.4 mg_{carbon} cm_{disk}^{-2}. The high catalyst loading, while suboptimal for kinetic ORR measurements,[16,29−31] guaranteed accurate determination of oxygen adsorption isotherms.

RESULTS

1. Cyclic Voltammetry of Oxygen on Vulcan-Supported Co and Fe Macrocycles. As shown in our previous paper,[16] cobalt phthalocyanine exhibits the most stable electrochemical behavior among the macrocycles selected for the present study. Therefore, it was selected to demonstrate the concepts and approaches applied to quantify the surface confinement of oxygen and major relationships governing the phenomenon.

Figure 1 shows selected RRDE voltammograms for ORR catalyzed by carbon (Vulcan XC72) supported CoPC (5.7%).

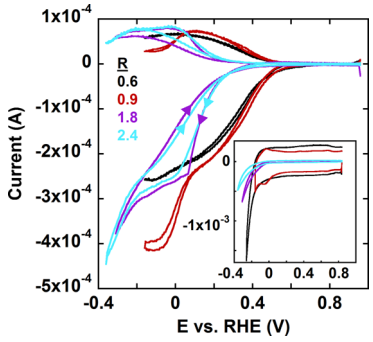

Figure 1. Background corrected RRDE voltammograms of oxygen saturated 0.5 mol dm^{-3} H_2SO_4 solution recorded for a 5.7% CoPC on Vulcan XC72. Total carbon loading 0.1 mg. Rotation rate 400 rpm. Scan rate 10 mV s^{-1}. Nafion contents (R) in the catalyst inks listed in the figure. Inset: cyclic voltammograms (100 mV s^{-1}) recorded for the same catalysts in deoxygenated 0.5 mol dm^{-3} H_2SO_4 solutions.

In agreement with our previous work,[16] higher Nafion contents (R ≥ 1.2, for picture clarity the data for $R = 1.2$ and $R = 1.5$ not shown in Figure 1) lead to significant ORR inhibition. The inhibition is associated with the blocking of the carbon surface by the hydrophobic component of Nafion,[16] as demonstrated by the significant suppression of the respective background currents (inset in Figure 1). Within the studied potential range (up to −0.36 V vs RHE), two oxygen reduction steps can be seen for R ≤ 0.9, but the inhibition of the reaction obscures the second reduction step at $R \geq 1.2$ (shown for $R \geq 1.8$ in Figure 1). A hysteresis is also observed between the forward and reverse scans of the voltammograms recorded for the inks, where the surface blocking takes place (Figure 1). The hysteresis was found to decrease with the electrode rotation rate (the rate of oxygen transport) and suggested that, in addition to the transport and charge transfer controlled oxygen reduction, transportless (rotation rate independent) phenomena contribute to the measured currents. The most likely among such phenomena is oxygen adsorption, which predominantly occurs under no current conditions (open circuit) and its reduction in the forward RRDE scan. It can lead to an enhancement of oxygen reduction currents in the forward scan and a much smaller (if any) current enhancement in the reverse (anodic) scan, which starts with no adsorbed oxygen.

That the current hysteresis in RRDE experiments was caused by oxygen adsorption was confirmed by standard cyclic voltammetry without electrode rotation. The stationary voltammograms recorded for the catalyst layers, where the hysteresis was observed in RRDE experiments exhibited very tall and rather symmetrical oxygen reduction peaks. The heights of those peaks increased with the electrode equilibration time at the open circuit, but stabilized after 5 min or shorter equilibration time at 400 rpm electrode rotation. Typical voltammograms recorded for catalyst layers containing various Nafion quantities after 5 min equilibration in fully oxygenated solutions and demonstrating the presence of surface confined oxygen for $R \geq 1.2$ are presented in Figure 2.

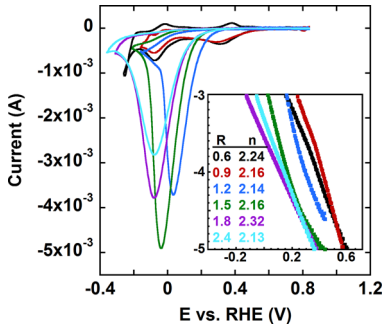

Figure 2. Cyclic voltammograms of oxygen saturated 0.5 mol dm^{-3} H_2SO_4 solution recorded for a 5.7% CoPC on Vulcan XC72. Total carbon loading 0.1 mg. Scan rate 500 mV s^{-1}. Equilibration time 5 min at 400 rpm. Nafion contents in the catalyst inks listed in the figure. Inset: logarithms of the kinetic ORR currents determined for the same catalysts from RRDE experiments at 400 rpm.[16] Nafion contents (R) in the catalyst inks and the respective numbers of electrons (n) transferred in the first ORR wave (determined from the respective ring currents at +1.2 V) are listed in the figure.

In agreement with the RRDE data (Figure 1), two oxygen reduction peaks corresponding to the two ORR steps can be seen in the voltammograms recorded for $R = 0.6$ and $R = 0.9$ (Figure 2). Two smaller reoxidation peaks are also seen in the reverse scans of these voltammograms. The ratios of the reverse to the forward peak currents were found to increase with scan rate and the reverse (anodic) peaks were almost absent at 100 mV s^{-1}. No mechanistic study of the reactions corresponding to the two red−ox systems was performed. However, the first CoPC reduction was found to correspond to around 100% generation of hydrogen peroxide (see the number of electrons

DOI: 10.1021/acs.jpcc.6b09523
J. Phys. Chem. C 2016, 120, 28038−28048

transferred in ORR listed in the inset in Figure 2) under RRDE conditions, whereas the number of electrons involved in the ORR at the potentials of the second step (visible in the studied potential range only at R ≤ 0.9) was higher than 2, but did not exceed 3. Upon the increase in R from 0.9 to 1.2, the two redox systems disappeared and were replaced by a large and relatively symmetrical oxygen reduction peak. Its position, height and width depended on Nafion concentration in the catalyst layer. The peak width increased with R, whereas the peak current increased upon transition from $R = 1.2$ to $R = 1.5$, but then decreased with further R increase (Figure 2). The peak position correlated with the ORR kinetics determined from the reverse scans of respective RRDE voltammograms (inset in Figure 2).

The voltammograms in Figure 2 were recorded after 5 min electrode equilibration (with 400 rpm rotation) at the open circuit potential in fully oxygenated solution. When applicable ($R \geq 1.2$), such conditions guaranteed equilibrium between the fully oxygenated solution and the surface confined oxygen as determined from a series of voltammetric experiments performed after different equilibration times. An identical procedure was used to determine the equilibration times required to reach the surface confinement equilibrium for all other catalysts and oxygen concentrations in this study.

A stepwise increase in the oxygen reduction peak current caused by the increase in Nafion content from $R = 0.9$ to $R = 1.2$ (Figure 2) indicates a significant increase in oxygen availability. Such an increase can only be explained by oxygen accumulation on the catalyst surface. The fast current decrease after the peak, observed for all Nafion contents corresponding to $R \geq 1.2$, is also concordant[32] with the above statement. While the observed changes leave little doubt that the major contribution to the measured currents at $R \geq 1.2$ originates from the reaction of surface confined oxygen, the measured currents are influenced by contributions from oxygen diffusing from the bulk of solution and the number of electrons involved in the reaction (inset in Figure 2). Similarly, the peak widths and positions depend on the actual charge transfer kinetics (inset in Figure 2). Such factors together with the adsorption kinetics have to be taken into account in order to correctly determine the equilibrium concentration of surface confined oxygen.

The reduction charge of surface confined oxygen can be determined using a relatively simple procedure whose principle is briefly described below. The total oxygen reduction current can be expressed as a sum of two contributions, one from oxygen diffusing from the bulk of solution and another corresponding to the surface confined oxygen. If the geometric surface density of active sites is sufficiently high to result in planar oxygen diffusion (confirmed in our previous paper[16]), the peak current (i_p) corresponding to the diffusion controlled process is expressed by the Nicholson and Shain equation.[33] On the other hand, the peak current for the reduction of surface confined oxygen will be described by an equation derived by Laviron.[32] These equations predict linear dependencies of the peak current on either the scan rate (v) for surface confined species[32] or its square root ($v^{1/2}$) for that diffusing from the bulk.[33] One can demonstrate that similar current (i) vs. v and current vs. $v^{1/2}$ relationships should hold for the respective processes at any fixed difference (ΔE) between the measured potential (E) and the respective peak potential (E_p):

$$i_{\Delta Esurface} = B_{\Delta Esurface} v \tag{1}$$

$$i_{\Delta Esolution} = B_{\Delta Esolution} v^{1/2} \tag{2}$$

where $i_{\Delta E\ \mathrm{surface}}$ and $i_{\Delta E\ \mathrm{solution}}$ represent the currents of the surface confined and the dissolved species, whereas the constants B are different for the diffusing and surface confined species and depend on the selected ΔE for each process. The integration of eqs 1 and 2 against time over ΔE results in

$$\int_{\Delta E} i_{surface} = G(\Delta E_{surface}) \tag{3}$$

$$\int_{\Delta E} i_{solution} = H(\Delta E_{solution}) v^{-1/2} \tag{4}$$

where G and H are ΔE-dependent constants. If a sufficiently wide range of ΔE on both sides of the surface reduction peak is selected, the integral in eq 3 becomes equal to the charge corresponding to the complete reduction of the surface confined species.

$$G(\Delta E \to \infty) \to Q_{surface} \tag{5}$$

The integration of an experimental voltammetric current containing the contributions from both adsorbed and dissolved species over a specific potential range fixes the $\Delta E_{\mathrm{solution}}$ and $\Delta E_{\mathrm{surface}}$ potential ranges. When the scan rate is changed, both of these ranges ($\Delta E_{\mathrm{solution}}$ and $\Delta E_{\mathrm{surface}}$ as measured vs the respective peak potentials) cannot be preserved simultaneously by adjusting the overall potential range ΔE because of the generally different E_p vs v relationships for surface confined[32] and dissolved[33] species. Consequently, the scan rate dependence of the electrolysis charge in a specific potential range ΔE measured vs. the peak potential cannot be expressed as an exact sum of eqs 3 and 4 with scan rate independent parameters G and H. However, if the potential range for the integration is significantly wider than the expected differences in the scan rate induced shifts of the peak potentials for the confined and dissolved species, an approximate relationship should still hold:

$$Q \approx Q_{surface} + H v^{-1/2} \tag{6}$$

The accuracy of eq 6 is expected to improve with scan rate, which reduces the second term in the equation corresponding to the contribution from the dissolved species. Moreover, an increase in the scan rate reduces interplay, if any, between the two components of the reduction current. The equation provides means to determine the reduction charge of the surface confined oxygen (Q_{surface}). The charges of interest can be extracted from the intercepts of the respective Q vs. $v^{-1/2}$ plots. The procedure was successfully used by us previously to determine the amount of surface confined oxygen for a pyrolyzed Fe/N/C catalyst.[1]

In Figure 3 are shown the voltammograms recorded for the 5.7% CoPC catalyst at different scan rates after 5 min equilibration at 400 rpm in fully oxygenated solution. As demonstrated by the virtually linear dependence between the peak current and the square root of the scan rate (top inset), the contribution of oxygen diffusing from the bulk to the measured currents is small. Consequently, eq 5 quite accurately describes the measured reduction charge Q, and the respective Q_{surface} can be reliably determined from a linear extrapolation of the measured charge Q against the inverse square root of time to zero. The corresponding linear relationship between Q and $v^{-1/2}$ is presented in the bottom inset in Figure 3.

The voltammetry of oxygen in the presence of other macrocycles in this study and at lower than saturated oxygen

DOI: 10.1021/acs.jpcc.6b09523
J. Phys. Chem. C 2016, 120, 28038−28048

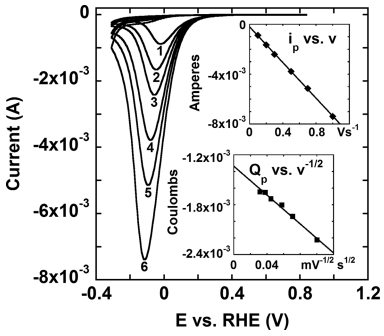

Figure 3. Cyclic voltammograms of oxygen saturated 0.5 mol dm^{-3} H_2SO_4 solution recorded for 5.7% CoPC on Vulcan XC72. Total carbon loading 0.1 mg. Equilibration time 5 min at 400 rpm. R = 1.8. Scan rate (mV s^{-1}): 100 (1), 200 (2), 300 (3), 500 (4), 700 (5), and 1000 (6). Top inset: peak current vs. scan rate showing the predominantly surface character of the oxygen reduction peak. Bottom inset: oxygen reduction charge plotted vs. inverse square root of the scan rate (see text for the charge determination methodology).

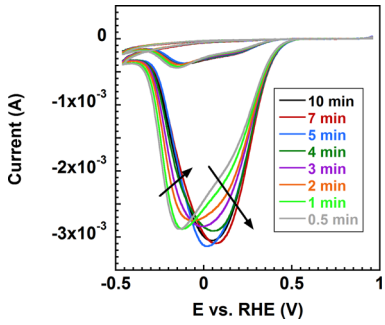

Figure 4. Two cycle voltammograms of oxygen-saturated 0.5 mol dm^{-3} H_2SO_4 solution recorded for 8.1% CoTPP on Vulcan XC72 after different equilibration times at 400 rpm. Total carbon loading 0.1 mg. R = 1.6. Scan rate 1000 mV s^{-1}.

concentrations was qualitatively similar to that described above for CoPC in the presence of oxygen saturated solutions (Figures 1–3). The respective ORR peaks were predominantly transport controlled for low Nafion contents in the catalyst layers and exhibited mostly diffusionless character at higher Nafion contents, which promoted self-assembly of Nafion. The results obtained for the iron macrocycles, especially FePCCl and FeTPPCl, were affected by the low complex durability under the ORR conditions and were excluded from quantitative analysis.

For the vast majority of catalyst layer compositions, including different macrocycles and Nafion contents, the kinetics of the processes leading to oxygen confinement was fast enough to guarantee the equilibrium surface concentration of oxygen in less than 5 min at 400 rpm. As no detailed kinetic studies were performed, no strictly quantitative conclusions regarding structural and catalyst concentration effects on the kinetics of the phenomenon could be reached. However, two observations were made. First, the kinetics of oxygen adsorption was faster for all studied systems than that observed by us previously for the previously mentioned pyrolyzed Fe/polyaniline catalyst.[1] Second, the peak potentials and widths for oxygen reduction correlated quite well with the kinetic ORR parameters determined for dissolved oxygen from the reverse (anodic) RRDE scans. However, the correlations were also influenced by the equilibration time, which moderately affected the shape and position of the reduction peaks. The phenomenon is illustrated in Figure 4 for 8.1% CoTPP catalyst (R = 1.6), where the observed changes were most prominent. They demonstrate an improvement in ORR catalysis of surface confined oxygen with the equilibration time. The enhancement of the apparent kinetics of the reduction of surface confined oxygen can hardly be attributed to changes in the intrinsic catalytic activity of the active sites. It most likely reflects potential-induced morphological changes in the catalyst layer, which affect the accessibility of the active sites and thus the apparent ORR kinetics.[16] The changes in morphology most likely involve Nafion[34] and the catalytically active molecules or their mobile fragments, *e.g.*, side phenyl groups in CoTPP. The changes did not measurably affect the reduction charges of oxygen corresponding to adsorption equilibrium.

2. Oxygen Adsorption on Macrocycle-Covered Vulcan XC72. The equilibrium surface concentrations of oxygen for all studied catalyst compositions were determined using the procedure demonstrated for 5.7% CoPC to measure charges of the adsorbed oxygen (Figure 3). The latter were subsequently corrected for the number of electrons involved in ORR to determine the number of moles of the adsorbed oxygen. In order to get accurate results, the number of electrons was determined from the respective forward (cathodic) RRDE scans, where surface confined oxygen contributed to the measured currents (Figure 1). Moreover, the same electrode equilibration times were used in both voltammetric and RRDE experiments and the number of electrons from RRDE experiments was averaged over the potential range used for the charge integration in voltammetry. The effects of various factors on oxygen adsorption were studied and included the amount of Nafion in the catalyst layer, the catalyst loading and composition, and the concentration of oxygen in solution.

2.1. Nafion Content and Active Site Concentration Effects on Oxygen Confinement on Vulcan-Supported Catalysts. The effect of Nafion quantity in the catalyst layer was studied for four catalysts containing CoPC as the active molecule and using exclusively oxygen saturated solutions. For three catalysts (1.7%, 5.7%, 13.6% CoPC), the desired quantities of Nafion were directly added to the catalyst inks, which were subsequently deposited on the RRDE tip. The fourth catalyst (5.4% CoPC) was deposited onto the electrode using an ink containing no Nafion. Subsequently, a small quantity of the solution obtained by 100-fold dilution with water of the commercial 5% Nafion was deposited on top of the dry catalyst layer to obtain the desired Nafion content in the layer. The surface concentrations of oxygen were determined using the procedure described in the previous section and assuming that the whole Vulcan XC72 surface area (~240 m^2 g^{-1}) participated in the oxygen confinement. The surface concentrations of oxygen are plotted in Figure 5 together with the respective backgrounds currents measured at 0.3 V vs. RHE and 100 mV s^{-1}. The data in Figure 5 demonstrate a correlation between the surface confinement of oxygen (Γ_{O_2}) and the suppression of the background currents by Nafion. As the latter results from self-assembly of Nafion on the carbon surface in the Nafion containing inks,[16] the observed changes in Γ_{O_2} and background currents have virtually stepwise character and the surface concentration of oxygen tends to stabilize around 2.4 × 10^{-11} mol cm^{-2} at high R, irrespective of the CoPC content in the catalyst. As demonstrated in our previous paper,[16] the actual number of active CoPC sites in the CoPC catalysts was

DOI: 10.1021/acs.jpcc.6b09523
J. Phys. Chem. C 2016, 120, 28038–28048

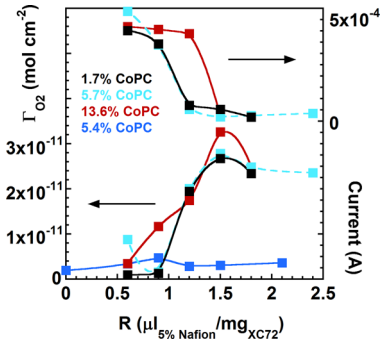

Figure 5. Oxygen surface concentrations (bottom) and voltammetric background currents measured at 0.3 V vs. RHE and 100 mV s^{-1} (top) plotted against Nafion content (R) in the catalyst layer. The background currents are sums of absolute currents measured in negative and positive scans. For the 5.4% CoPC catalyst, Nafion was deposited on top of the Nafion free catalyst layer as an aqueous solution obtained by 100-fold dilution of the commercial 5% solution.

not proportional to the mass percentage of CoPC due to carbon/CoPC agglomeration phenomena. However, the number of active sites per mass of the carbon support for the 13.6% CoPC catalyst can be estimated from the background currents and the measured ORR activities as up to 3 times higher than that for the catalysts with 1.7% and 5.7% CoPC. Consequently, a 3-fold increase in the number of active CoPC sites has virtually no effect on the observed surface confinement of oxygen.

2.2. Oxygen Adsorption Isotherms for Vulcan-Supported Macrocyclic Complexes and Their Mixtures with the Respective Ligands. Oxygen adsorption isotherms were determined for selected macrocyclic complexes and mixtures of the complexes with their respective ligands at selected Nafion contents (R) guaranteeing the maximum carbon surface blockage by Nafion but not allowing for the formation of a bulk Nafion phase in the catalyst layer.[16] The surface concentrations of oxygen were measured for four different oxygen concentrations in solution using the procedure outlined above. Irrespective of the catalyst layer composition, a linear relationship was found between the surface (Γ) and bulk oxygen concentration. Such a relationship is described by the Henry's adsorption isotherm, a limiting form of the Langmuir isotherm for low surface concentrations, where the adsorbed molecules virtually do not interact with each other. A typical adsorption isotherm is presented in Figure 6, whereas the numerical data obtained for all macrocyclic catalysts are

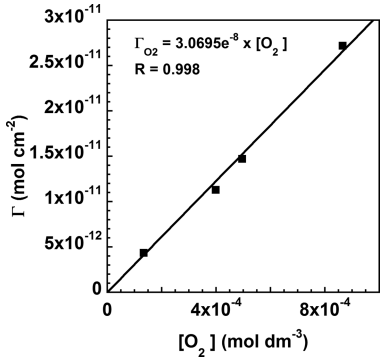

Figure 6. Oxygen adsorption isotherm for 8.1% CoTPP catalyst (R = 1.6) in 0.5 mol dm^{-3} H_2SO_4 solution.

collected in Table 1. Inspection of the data in Table 1 reveals the lack of major effects of the macrocyclic complexes and their ligands on the surface confinement of oxygen. The nonspecific character of the confinement indicates that neither the complexes nor their bare ligands play an important role in the phenomenon. On the other hand, the correlation between the surface confinement of oxygen and the self-assembly of Nafion implies that the latter is exclusively responsible for the accumulation of oxygen on the surface. The only role played by the active centers in the voltammetry of surface confined oxygen is its reduction. In order to confirm the correctness of the above hypothesis, a series of experiments were performed with three carbon-supported Pt catalysts. Two of them (Pt4.8V - 4.8% Pt on Vulcan and Pt4.8G - 4.8% on graphitized carbon) were previously demonstrated to promote self-assembly of Nafion,[16] whereas the third one (Pt20V - 20% Pt on Vulcan) did not support Nafion adsorption up to and including R = 2.7. The results obtained for the Pt catalysts are summarized in the following section.

3. Oxygen Confinement in Carbon-Supported Pt Catalysts. Figure 7 shows background corrected voltammograms (100 mV s^{-1}) of oxygen reduction on three Pt catalysts after 5 min equilibration in oxygen saturated solutions. Only a slight distortion of the diffusion controlled ORR peak is observed for Pt20 V with high Nafion content (R = 1.8), whereas the voltammograms recorded for the two low Pt content catalysts exhibit significantly higher peaks whose shapes reveal their predominantly surface controlled character. There are also differences between the voltammograms recorded for these two catalysts. The voltammogram obtained for Pt4.8G exhibits higher currents in the whole cathodic potential range than that recorded for its counterpart with nongraphitized support (Vulcan). The actual quantities of surface confined oxygen for the three Pt catalysts and different Nafion contents were obtained from respective oxygen reduction charge vs. $\nu^{-1/2}$ plots corrected by the number of electrons transferred in ORR. They are compared with the data obtained for the macrocyclic catalysts in Figure 8. The quantities of surface confined oxygen in Figure 8 are referred to the mass of the carbon support rather than to its surface area, because the metal particles in the different Pt catalysts occupy different and not exactly known fractions of the support surface areas and are affected (Pt4.8V and Pt4.8G) or not (Pt20V)[16] by Nafion self-assembly. Moreover, the surface properties of carbon supports do affect the distribution of Pt particles in supported catalysts,[35,36] which may influence Nafion self-assembly in a similar way to that observed for Pt20V.

Figure 8 reveals that almost two times higher quantity of oxygen can be confined at the interfaces between the graphitized carbon and Nafion (Pt4.8G) than between Vulcan and Nafion (Pt4.8V) even though the specific surface area of Vulcan (205−250 m^2 g^{-1})[18−21] is significantly higher than that of Pt4.8G (157 m^2 g^{-1}). A comparable amount of oxygen per mass of the carbon support to that measured for Pt4.8G can be confined at the Vulcan/Nafion interface for the studied macrocyclic catalysts. On the other hand, almost no oxygen can be confined at the Vulcan/Nafion interface in Pt20V catalyst.

The favorable role of graphitic surfaces in Nafion induced confinement of oxygen correlates with the attractive London dispersion interactions between the π electrons of the oxygen double bond and those delocalized over aromatic graphitic surfaces.[37,38] The reasons why the London forces are

DOI: 10.1021/acs.jpcc.6b09523
J. Phys. Chem. C 2016, 120, 28038−28048

Table 1. Equilibrium (Henry's) Constants and Concentrations of Surface-Confined Oxygen Measured for Co and Fe Macrocyclic Complexes Adsorbed on Vulcan XC72 in the Presence of Self-Assembled Nafion Layers[a]

catalyst	R (μL (5% nafion)/ mg (XC72))	Henry's constant (cm)	correlation coefficient	Γ_{meas}[b] (mol cm^{-2})	Γ_{calc}[c] (mol cm^{-2})
6.4% CoPC	1.3	(2.63 ± 0.04) × 10^{-5}	0.998	2.22 × 10^{-11}	2.28 × 10^{-11}
5.0% CoPC + 5.0% PC	1.3	(2.36 ± 0.55) × 10^{-5}	0.732	2.10 × 10^{-11}	2.04 × 10^{-11}
6.9% CoOEP + 6.5% OEP	1.5	(3.20 ± 0.08) × 10^{-5}	0.998	2.83 × 10^{-11}	2.77 × 10^{-11}
8.1% CoTPP	1.6	(3.07 ± 0.06) × 10^{-5}	0.998	2.72 × 10^{-11}	2.66 × 10^{-11}
6.0% CoTPP + 6.2% TPP	1.4	(3.01 ± 0.12) × 10^{-5}	0.991	2.56 × 10^{-11}	2.61 × 10^{-11}
9.8% FeOEPCl	1.7	(2.56 ± 0.26) × 10^{-5}	0.960	2.53 × 10^{-11}	2.22 × 10^{-11}

[a]Surface concentrations calculated assuming that the entire carbon surface participates in the surface confinement of oxygen. [b]Measured in O_2 saturated solution (8.65 × 10^{-4} mol dm^{-3}) at 2100 m above sea level [c]Calculated from the adsorption isotherm for O_2 saturated solution (8.65 × 10^{-4} mol dm^{-3}) at 2100 m above sea level

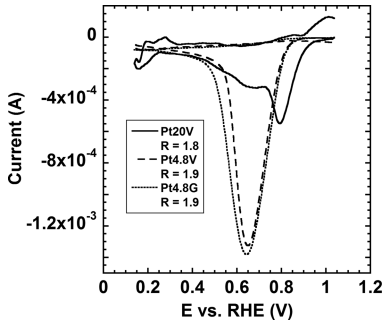

Figure 7. Background corrected cyclic voltammograms of oxygen saturated 0.5 mol dm-3 H_2SO_4 solution recorded for three Pt catalysts after 5 min equilibration at 400 rpm. Scan rate 100 mV s^{-1}. Nafion contents in the catalyst layers listed in the legend.

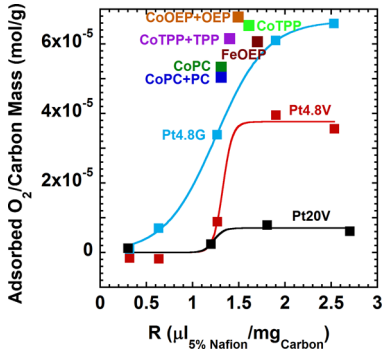

Figure 8. Molar concentrations of surface confined oxygen per gram of catalyst support in oxygen saturated 0.5 mol dm^{-3} H_2SO_4 solution plotted against Nafion content in the catalyst layer for three Pt catalysts on different carbon supports and six macrocyclic complexes of Co and iron supported on Vulcan XC72. Macrocyclic catalyst compositions: CoPC (6.4%), CoPC + PC (5.0% CoPC, 5.0% PC), FeOEP (9.8% FeOEPCl), CoTPP (8.1%), CoTPP + TPP (6.0% CoTPP, 6.2% TPP), and CoOEP + OEP (6.9% CoOEP, 6.5% OEP).

insufficiently strong to produce measurable quantities of surface confined oxygen at the carbon/aqueous solution interfaces containing no Nafion will be further discussed in the Discussion.

4. ORR Catalyzed by Nafion-Coated CoPC/HOPG and Pt/HOPG. The results of our previous study[16] indicate that Nafion self-assembly is promoted by graphitic surfaces, but it spills over adjacent nongraphitic surfaces to form a complete monolayer coverage of the studied carbon supports. On the other hand, the data presented in the previous sections (Figure 8) suggest that oxygen accumulates predominantly, if not exclusively, at the interfaces between graphitic surfaces and the hydrophobic component of self-assembled Nafion.[16]

Highly ordered pyrolytic graphite (HOPG) with its almost atomically flat graphitic surface and demonstrated ability to promote self-assembly of Nafion[16,39] seemed to offer a unique opportunity to determine the quantitative relationship between the concentration of surface confined oxygen and the real graphitic surface area from ORR measurements. The expected contributions from surface confined oxygen in total oxygen reduction currents (charges) are much smaller for HOPG than those observed for the high surface area carbons. If 100% of the Vulcan surface area contributed to the oxygen confinement demonstrated in the previous sections, one could expect the geometric surface area charge density resulting from the reduction of oxygen confined on the surface of HOPG to be only around 10 μC cm^{-2}. However, as proven by the results obtained for Pt4.8G, only a fraction of Vulcan surface area contributes to oxygen confinement. That finding gave us hope that the quantity of oxygen confined at HOPG/Nafion interfaces would be higher than 10 μC cm^{-2} and thus accurately measurable.

HOPG electrodes containing CoPC and Pt as oxygen reduction catalysts were prepared. The procedure to deposit Pt nanoparticles on HOPG is described in the Experimental Section. The method used to deposit CoPC on the graphite was as follows. A green and stable colloidal CoPC solution of known concentration in DCM was diluted with pure DCM to obtain a virtually colorless ~3.6 × 10^{-5} mol dm^{-3} CoPC suspension (or solution?) in DCM, which was subsequently deposited onto an HOPG disk and allowed to dry to produce a catalyst layer containing ~2 × 10^{-9} mol cm^{-2} CoPC (nominally in excess of 200 monolayers[40]) on the HOPG surface. As opposed to alcoholic (IPA and methanol) solutions of the other studied macrocycles, DCM was not causing Kapton delamination from HOPG. The CoPC catalyst layers fabricated in the above way were found to lose almost 100% of their initial catalytic activity during a single voltammetric scan in oxygenated H_2SO_4 solutions. Their stability was significantly improved after the deposition of thin Nafion films, but even then it was impossible to measure both the background and the ORR currents at more than a single scan rate without a visible loss in the electrode activity. Consequently, we abandoned any quantitative comparison between uncoated and Nafion coated electrodes.

In Figure 9 are shown background corrected voltammograms (first scans) of oxygen recorded at 1 V/s for HOPG-supported CoPC and Pt, coated with thin Nafion films after 5 min (CoPC) or 10 min (Pt) equilibration at their open circuit potentials in fully oxygenated H_2SO_4 solution. Such equilibra-

DOI: 10.1021/acs.jpcc.6b09523
J. Phys. Chem. C 2016, 120, 28038−28048

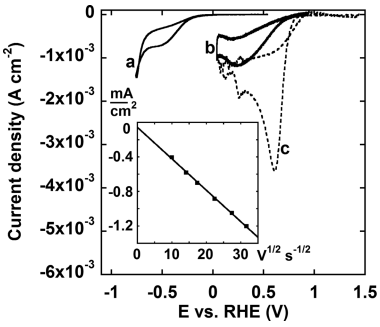

Figure 9. Background corrected cyclic voltammograms of oxygen saturated 0.5 mol dm^{-3} H_2SO_4 solution recorded for 2 × 10^{-9} mol cm^{-2} CoPC (a) and Pt nanoparticles (0.024 cm^2 surface area, b) deposited on ∼4.8 mm HOPG disk and covered with a self-assembled Nafion film as well as for an uncoated 1.6 mm Pt disk (c). Scan rate 1 V s^{-1}. Inset: peak current density for the HOPG/Pt/Nafion electrode plotted against the square root of scan rate.

tion times deemed sufficient to guarantee an equilibrium between the dissolved and surface-confined oxygen. For comparison, a voltammogram measured under the identical conditions using an uncoated 1.6 mm Pt disk (0.02 cm^2) is also shown in Figure 9.

As seen in Figure 9, the peak current densities for both HOPG supported catalysts are significantly lower than that measured for solid Pt. While the effect could be in part accounted for by the lower ORR Tafel slopes measured for the HOPG-supported catalysts, it is believed to predominantly result from the spatial isolation of numerous active centers. When the distances between the active centers (particles) are larger than the diameters of the respective diffusion layers around them, the centers act as individual ultramicro- (or rather nano-) electrodes. The ORR current for such centers, while enhanced by the hemispherical oxygen diffusion, will be lower than expected from the total geometrical surface area they occupy and will exhibit a steady state character. The shape of voltammograms in Figure 9 suggests a significantly nonuniform active site distribution on the HOPG surface. In some areas, the active centers are close enough to form a "uniformly" active surface. Such areas are responsible for planar oxygen diffusion toward the electrode and the presence of the oxygen reduction peak current proportional to the square root of the scan rate (inset in Figure 9). In other areas, where the active particles are far apart, a hemispherical diffusion to the individual sites occurs and contributes to the lower and time (scan rate) independent ORR currents (nonzero intercept of the peak current vs square root of the scan rate in the inset in Figure 9). One can imagine that oxygen potentially confined at the HOPG/Nafion interface in the areas surrounding the isolated Pt particles can no longer be reduced without a (surface) diffusion step. Therefore, the separation of the reduction charges corresponding to the surface confined and bulk oxygen, which was implemented in eq 6, can no longer be used to determine the quantity of surface confined oxygen from the experimental results shown in Figure 9. The determination of conditions necessary to achieve a uniform and sufficiently dense distribution of platinum particles on HOPG, which would enable the accurate determination of oxygen quantity trapped in the hydrophobic Nafion component at its interface with HOPG is the subject of a forthcoming study.

DISCUSSION

The results obtained for the two Pt catalysts with low metal content show that the amount of surface confined oxygen in the presence of self-assembled Nafion increases with the degree of surface graphitization. This finding indicates the presence of attractive interactions between O_2 molecules and graphitic surfaces, in agreement with the results of density functional theory (DFT) and self-consistent field (SCF) *ab initio* calculations performed for oxygen/graphite[38] and oxygen/benzene[37] systems, respectively. However, these interactions are too weak to cause O_2 adsorption in absence of self-assembled Nafion films. The calculated energies of these interactions are ∼0.11 eV ($\Delta H^0 \approx -10.6$ kJ mol^{-1}) for O_2-graphite[38] and ∼1.5 kcal mol^{-1} ($\Delta H^0 \approx -6.3$ kJ mol^{-1}) for O_2−C_6H_6.[37] The standard entropy contribution ($-T\Delta S^0$) for the transition from gaseous[41] to adsorbed[42] oxygen can be calculated as ∼+26.5 kJ mol^{-1} at 298 K. The free energy of molecular oxygen dissolved in 0.5 mol dm^{-3} H_2SO_4 is higher by 9.1 kJ mol^{-1} than that in the gas phase, as estimated from the oxygen solubility in that medium.[1] In conclusion, the estimated free energy of oxygen transfer from the solution phase (0.5 M H_2SO_4) to the adsorbed state on a graphitic surface can be calculated as −10.6 + 26.5 − 9.1 = 6.8 kJ mol^{-1}. The obtained number is positive, which explains why no oxygen adsorption can be observed in absence of Nafion self-assembly. The situation changes when a self-assembled monolayer of the ionomer occupies the carbon/solution interface. The free energy of oxygen adsorption on graphitic surfaces in the presence of self-assembled Nafion cannot be accurately determined if the actual graphitic surface area is not known. However, a realistic estimate of that energy can still be made using reasonable assumptions. First, let us assume that the maximum surface concentration of oxygen on a graphitic surface is equal to that of "benzene" rings[37] in graphene (∼3.2 × 10^{-9} mol cm^{-2}, as calculated from graphene morphology[43,44]). Second, let us assume that the graphitic surface area of the Pt4.8G catalyst constitutes between (unlikely low) 10% and 100% of the total surface area (Figure 8). The free energy of adsorption calculated for the above surface area limits using a Langmuir adsorption isotherm equals −12.7 and −6.7 kJ mol^{-1} for the 10% and 100% graphitic surface area contribution, respectively.

While the role of self-assembled Nafion in the surface confinement of oxygen is indisputable, it calls for an explanation. Specifically, a question arises whether the oxygen confinement can be explained by simple differences in oxygen solubility in Nafion and in 0.5 mol dm^{-3} H_2SO_4 solutions. Bulk Nafion is known to exhibit different oxygen solubilities in its hydrophobic and hydrophilic components, the former showing a significantly higher oxygen affinity than the latter.[45−47] The self-assembled backbone of Nafion[16] forms a continuous nanophase, similar to that in the bulk ionomer,[48] which could promote oxygen accumulation. If it is assumed that the oxygen solubility in such a nanophase is equal to that in Teflon[49] and the thickness of the Teflon like layer is around 0.3 nm,[16] one gets ∼2.2 × 10^{-13} mol cm^{-2} for the expected surface concentration of oxygen in a self-assembled Nafion layer, which is at least 100 times lower than what observed experimentally (Table 1). The finding demonstrates that self-assembled Nafion and graphitic surface are both necessary for the surface confinement of oxygen to occur. The same conclusion could have already been reached from the

DOI: 10.1021/acs.jpcc.6b09523
J. Phys. Chem. C 2016, 120, 28038−28048

qualitative observation that oxygen confinement occurs only in the presence of self-assembled Nafion and increases with the degree of carbon surface graphitization.

The limiting values (−6.7 to −12.7 kJ mol^{-1}, calculated above for Pt4.8G) of the free energy of oxygen adsorption exclude the presence of even the weakest covalent bonding between oxygen and carbon and/or Nafion. The lack of such bonding, while intuitively understood and expected, can also be inferred from the electrochemical data, which demonstrate that the reduction of surface confined oxygen occurs at the overpotentials virtually identical with those measured for oxygen diffusing from the bulk of solution (see Figures 1 and 2).

As opposed to strongly hydrophobic graphitic surfaces,[50,51] amorphous carbon surfaces lack highly delocalized π electrons responsible for surface hydrophobicity. The atoms with unpaired electrons on amorphous surfaces easily undergo oxidation, which makes the surface even less hydrophobic due to the presence of oxidized functional groups.[52] Such surfaces are not expected to promote self-assembly of Nafion through its hydrophobic component, as observed previously[16] and in the present study. To the contrary, if the surface is sufficiently hydrophilic, self-assembly of Nafion through its hydrophilic component may occur.[17] Consequently, graphitized carbon surfaces attract the hydrophobic Nafion component much stronger than amorphous surfaces and are most likely exclusively responsible for the self-assembly of Nafion and the resulting surface confinement of oxygen.

The responsibility of hydrophobic interactions between graphitic carbon surfaces and the hydrophobic Nafion component for the self-assembly of Nafion on the carbon-supported catalysts and the resulting surface confinement of oxygen are intuitively understood. However, the potential role of other factors in both phenomena should not be underestimated. It cannot be assumed that the entire graphitic surface of a highly dispersed carbonaceous material actively participates in these phenomena. As demonstrated above, the presence of hydrophilic Pt particles in Pt catalysts lowers the extent of Nafion self-assembly[16] and the oxygen confinement. The magnitude of the effect is expected to depend on the distribution of the catalyst particles between the hydrophobic and hydrophilic fractions of the carbon surface. Moreover, a complex morphology of high surface area carbon particles may hamper the self-assembly, as Nafion molecules, in spite of their flexibility, cannot follow all microstructural features of the carbon surface. As previously suggested,[16] the factor determining Nafion self-assembly is the graphitic fraction of the surface on the carbon particle perimeter. Consequently, it is rather the graphitic fraction of the "geometric" particle surface area, which is responsible for the self-assembly and oxygen confinement. However, the latter might be enhanced by entrapment of O_2 molecules in the nanopores of carbon particles.

The lack of any direct involvement of the metal centers of the macrocyclic complexes in the surface confinement of oxygen seems to contrast our previous conclusions regarding heat treated Fe/polyaniline composites.[1] A correlation between the surface density of the active sites and the amount of surface confined oxygen was detected by us for those catalysts and attributed to oxygen adsorption occurring either directly on the active sites or in their immediate vicinity. The disparity between the previous[1] and the current conclusions is most likely superficial. In reality, both results reflect the same phenomenon. As frequently postulated,[3−5] the FeN_4 active sites in pyrolyzed Fe/N/C composites are embedded in graphene planes and therefore their number is likely to correlate with the degree of surface graphitization. In turn, the latter is a key factor determining the extent of Nafion self-assembly and the resulting oxygen confinement, whereas the role of the very active sites in the reduction of surface confined oxygen is exclusively the electrochemical process, but not the adsorption itself. Such explanation of the previous results[1] remains in agreement with the insensitivity of the surface confinement of oxygen to the nature of the active site demonstrated in this paper.

As previously noted,[16] the only active sites in a catalyst that can participate in ORR in the presence of Nafion self-assembly are those with direct access to the electrolyte. Hydrophobic macrocyclic complexes, such as those used in the present study, likely adsorb exclusively on carbon graphitic planes[53] and are especially susceptible to blocking by the Nafion hydrophobic component and to complete elimination from the electrocatalysis. Therefore, any ORR results obtained for Nafion containing catalyst inks have to be first examined for possible Nafion self-assembly, which may lead to a strong inhibition of the reaction but also to its apparent "acceleration" resulting from possible surface confinement of oxygen. The latter will not be visible in RRDE data obtained using a staircase methodology,[1] which allows for truly steady state measurement. Catalyst supports such as graphitized carbons, graphene and carbon nanotubes are expected to be especially susceptible to the inhibition and oxygen confinement phenomena originating from Nafion self-assembly. On the other hand, hydrophilic groups (*e.g.*, carboxyl, carbonyl, or hydroxyl) present on the surface of carbon support may decrease or, in extreme cases, even prevent Nafion self-assembly and the resulting ORR inhibition and surface confinement of oxygen.

Finally, a few remarks can be made on the potential effects of surface confinement of oxygen on the performance of polymer electrolyte fuel cells (PEFCs) employing Nafion and carbon-supported catalysts. As demonstrated above, surface confinement of oxygen emerges only in the presence of Nafion self-assembled through its hydrophobic component on carbon nanoparticles. To our knowledge, no such phenomenon has been reported for fuel cell catalyst layers. It is a matter of speculation whether self-assembly of Nafion has not yet been noticed or simply cannot exist in such layers due to their different morphologies. The latter originate from two major factors: (1) the presence of bulk Nafion phase resulting from significantly higher Nafion loadings and (2) thermal treatment.[54−56] Nevertheless, if the phenomenon can exist in fuel cell catalyst layers, it cannot markedly affect a continuous cell operation, since it involves a small finite quantity of oxygen, which is quickly consumed in the ORR. In intermittent fuel cell operation, a limited power boost might be expected when the fuel cell current is ramped from zero to its desired level.

In principle, the largest potential effects of surface confined oxygen on the fuel cell durability may be expected at open circuit.[57] This is because (1) the total oxygen concentration in the cathode layer is highest under such conditions and (2) oxygen crossover and the heat and hydrogen peroxide generating hydrogen combustion on the anode side may occur.[57] However, surface-confined oxygen is not a free species. When no net current flows through the fuel cell, the quantity of surface-confined oxygen remains constant and determined by the (controlled) pressure in the cathode compartment. Consequently, the flux of oxygen through the membrane will

DOI: 10.1021/acs.jpcc.6b09523
J. Phys. Chem. C 2016, 120, 28038−28048

not be affected by the quantity of surface confined oxygen and so will not be the membrane deterioration.[57]

CONCLUSIONS

- Self-assembly of Nafion through its hydrophobic backbone on high surface area carbon supports of oxygen reduction catalysts promotes oxygen accumulation (surface confinement) at the interface between the ionomer and graphitic surfaces of the carbon support
- The estimated free energy of surface confinement of oxygen indicates that oxygen trapped between graphitic surfaces and self-assembled Nafion backbone interacts with both components via London dispersion forces
- Surface confinement of oxygen may lead to erroneous determination of catalytic activities of oxygen reduction catalysts in aqueous media using a linear sweep RDE (RRDE) voltammetry. The problem can be mitigated if staircase voltammetry is applied
- Surface confinement of oxygen can be potentially applied as a measure of the degree of carbon surface graphitization

AUTHOR INFORMATION

Corresponding Author

*(J.C.) E-mail: jerzy@lanl.gov.

ORCID

Jerzy Chlistunoff: 0000-0002-8583-0243

Notes

The authors declare no competing financial interest.

ACKNOWLEDGMENTS

The financial support from the UC Office of the President (Lab Fees Research Program, Grant ID No. 12-LR-237440) is gratefully acknowledged.

REFERENCES

(1) Chlistunoff, J. RRDE and Voltammetric Study of ORR on Pyrolyzed Fe/Polyaniline Catalyst. On the Origins of Variable Tafel Slopes. *J. Phys. Chem. C* **2011**, *115*, 6496−6507.

(2) Liu, Y. Is the Free Energy Change of Adsorption Correctly Calculated? *J. Chem. Eng. Data* **2009**, *54*, 1981−1985.

(3) Lefèvre, M.; Dodelet, J. P.; Bertrand, P. Molecular Oxygen Reduction in Pem Fuel Cells: Evidence for the Simultaneous Presence of Two Active Sites in Fe-Based Catalysts. *J. Phys. Chem. B* **2002**, *106*, 8705−8713.

(4) Koslowski, U. I.; Abs-Wurmbach, I.; Fiechter, S.; Bogdanoff, P. Nature of the Catalytic Centers of Porphyrin-Based Electrocatalysts for the ORR: A Correlation of Kinetic Current Density with the Site Density of Fe-N_4 Centers. *J. Phys. Chem. C* **2008**, *112*, 15356−15366.

(5) Schulenburg, H.; Stankov, S.; Schünemann, V.; Radnik, J.; Dorbandt, I.; Fiechter, S.; Bogdanoff, P.; Tributsch, H. Catalysts for the Oxygen Reduction from Heat-Treated Iron(III) Tetramethoxyphenylporphyrin Chloride: Structure and Stability of Active Sites. *J. Phys. Chem. B* **2003**, *107*, 9034−9041.

(6) Chlistunoff, J.; Sansiñena, J.-M. Effects of Axial Coordination of the Metal Center on the Activity of Iron Tetraphenylporphyrin as a Nonprecious Catalyst for Oxygen Reduction. *J. Phys. Chem. C* **2014**, *118*, 19139−19149.

(7) Matter, P. H.; Zhang, L.; Ozkan, U. S. The Role of Nanostructure in Nitrogen-Containing Carbon Catalysts for the Oxygen Reduction Reaction. *J. Catal.* **2006**, *239*, 83−96.

(8) Maldonado, S.; Stevenson, K. J. Influence of Nitrogen Doping on Oxygen Reduction Electrocatalysis at Carbon Nanofiber Electrodes. *J. Phys. Chem. B* **2005**, *109*, 4707−4716.

(9) Ramaswamy, N.; Tylus, U.; Jia, Q.; Mukerjee, S. Activity Descriptor Identification for Oxygen Reduction on Nonprecious Electrocatalysts: Linking Surface Science to Coordination Chemistry. *J. Am. Chem. Soc.* **2013**, *135*, 15443−15449.

(10) Zagal, J. H.; Gulppi, M.; Isaacs, M.; Cárdenas-Jirón, G.; Aguirre, M. J. Linear Versus Volcano Correlations between Electrocatalytic Activity and Redox and Electronic Properties of Metallophthalocyanines. *Electrochim. Acta* **1998**, *44*, 1349−1357.

(11) Shi, Z.; Zhang, J. Density Functional Theory Study of Transitional Metal Macrocyclic Complexes' Dioxygen-Binding Abilities and Their Catalytic Activities toward Oxygen Reduction Reaction. *J. Phys. Chem. C* **2007**, *111*, 7084−7090.

(12) Viswanathan, V.; Hansen, H. A.; Rossmeisl, J.; Nørskov, J. K. Universality in Oxygen Reduction Electrocatalysis on Metal Surfaces. *ACS Catal.* **2012**, *2*, 1654−1660.

(13) Stamenkovic, V.; Mun, B. S.; Mayrhofer, K. J. J.; Ross, P. N.; Markovic, N. M.; Rossmeisl, J.; Greeley, J.; Nørskov, J. K. Changing the Activity of Electrocatalysts for Oxygen Reduction by Tuning the Surface Electronic Structure. *Angew. Chem., Int. Ed.* **2006**, *45*, 2897−2901.

(14) Bard, A. J.; Faulkner, L. R. *Electrochemical Methods: Fundamentals and Applications*, 2nd ed.; John Wiley & Sons: New York, 2001; p 833.

(15) Christie, J. H.; Lingane, P. J. Theory of Staircase Voltammetry. *J. Electroanal. Chem.* **1965**, *10*, 176−182.

(16) Chlistunoff, J.; Sansiñena, J.-M. On the Use of Nafion® in Electrochemical Studies of Carbon Supported Oxygen Reduction Catalysts in Aqueous Media. *J. Electroanal. Chem.* **2016**, *780*, 134−146.

(17) Paul, D. K.; Karan, K.; Docoslis, A.; Giorgi, J. B.; Pearce, J. Characteristics of Self-Assembled Ultrathin Nafion Films. *Macromolecules* **2013**, *46*, 3461−3475.

(18) Hasche, F.; Oezaslan, M.; Strasser, P. Activity, Stability and Degradation of Multi Walled Carbon Nanotube (MWCNT) Supported Pt Fuel Cell Electrocatalysts. *Phys. Chem. Chem. Phys.* **2010**, *12*, 15251−15258.

(19) Andersen, S. M.; Borghei, M.; Dhiman, R.; Jiang, H.; Ruiz, V.; Kauppinen, E.; Skou, E. Interaction of Multi-Walled Carbon Nanotubes with Perfluorinated Sulfonic Acid Ionomers and Surface Treatment Studies. *Carbon* **2014**, *71*, 218−228.

(20) Wang, G.; Sun, G.; Zhou, Z.; Liu, J.; Wang, Q.; Wang, S.; Guo, J.; Yang, S.; Xin, Q.; Yi, B. Performance Improvement in Direct Methanol Fuel Cell Cathode Using High Mesoporous Area Catalyst Support. *Electrochem. Solid-State Lett.* **2005**, *8*, A12−A16.

(21) Garron, A.; Bennici, S.; Auroux, A. In Situ Generated Catalysts for $NaBH_4$ Hydrolysis Studied by Liquid-Phase Calorimetry: Influence of the Nature of the Metal. *Appl. Catal., A* **2010**, *378*, 90−95.

(22) Kinoshita, K. *Carbon: Electrochemical and Physicochemical Properties*; John Wiley & Sons: New York, 1988.

(23) Pahalagedara, L.; Sharma, H.; Kuo, C. H.; Dharmarathna, S.; Joshi, A.; Suib, S.; Mhadeshwar, A. B. In *Influence of Particle Size and Microstructure on the Oxidation Behavior of Carbon Blacks and Diesel Soot*; Presented at the 2012 AIChE Annual Meeting, Pittsburgh, PA, 2012; p 5.

(24) Ju, W.; Brulle, T.; Favaro, M.; Perini, L.; Durante, C.; Schneider, O.; Stimming, U. *ChemElectroChem* **2015**, *2*, 547−558.

(25) Durst, J.; Siebel, A.; Simon, C.; Hasché, F.; Herranz, J.; Gasteiger, H. A. New Insights into the Electrochemical Hydrogen Oxidation and Evolution Reaction Mechanism. *Energy Environ. Sci.* **2014**, *7*, 2255−2260.

(26) Durst, J.; Simon, C.; Hasché, F.; Gasteiger, H. A. Hydrogen Oxidation and Evolution Reaction Kinetics on Carbon Supported Pt, Ir, Rh, and Pd Electrocatalysts in Acidic Media. *J. Electrochem. Soc.* **2015**, *162*, F190−F203.

(27) Guzmán-Blas, R.; Suazo-Dávila, D.; Velez, C. A.; Daza, C. E.; Stacchiola, D. J.; Sasaki, K.; Senanayake, S. D.; Johnston-Peck, A. C.; Molina, R.; Cabrera, C. R. EDTA-Ce(III) Modified Pt Vulcan XC-72 Catalyst Synthesis for Methanol Oxidation in Acid Solution. *Electrocatalysis* **2014**, *5*, 50−61.

DOI: 10.1021/acs.jpcc.6b09523
J. Phys. Chem. C 2016, 120, 28038−28048

(28) Scherrer, P. Bestimmung der Grösse und der Inneren Struktur von Kolloidteilchen Mittels Röntgenstrahlen. *Nachrichten von der Gesellschaft der Wissenschaften, Göttingen* **1918**, 98−100.
(29) Gloaguen, F.; Convert, P.; Gamburzev, S.; Velev, O. A.; Srinivasan, S. An Evaluation of the Macro-Homogeneous and Agglomerate Model for Oxygen Reduction in PEMFCs. *Electrochim. Acta* **1998**, *43*, 3767−3772.
(30) Guilminot, E.; Corcella, A.; Chatenet, M.; Maillard, F. Comparing the Thin-Film Rotating Disk Electrode and the Ultra-microelectrode with Cavity Techniques to Study Carbon-Supported Platinum for Proton Exchange Membrane Fuel Cell Applications. *J. Electroanal. Chem.* **2007**, *599*, 111−120.
(31) Perry, M.; Newman, J.; Cairns, E. J. Mass Transport in Gas-Diffusion Electrodes: A Diagnostic Tool for Fuel-Cell Cathodes. *J. Electrochem. Soc.* **1998**, *145*, 5−15.
(32) Laviron, E. General Expression of the Linear Potential Sweep Voltammogram in the Case of Diffusionless Electrochemical Systems. *J. Electroanal. Chem. Interfacial Electrochem.* **1979**, *101*, 19−28.
(33) Nicholson, R. S.; Shain, I. Theory of Stationary Electrode Polarography. Single Scan and Cyclic Methods Applied to Reversible, Irreversible, and Kinetic Systems. *Anal. Chem.* **1964**, *36*, 706−723.
(34) Chlistunoff, J.; Pivovar, B. Effects of Ionomer Morphology on Oxygen Reduction on Pt. *J. Electrochem. Soc.* **2015**, *162*, F890−F900.
(35) Ferreira-Aparicio, P.; Folgado, M. A.; Daza, L. High Surface Area Graphite as Alternative Support for Proton Exchange Membrane Fuel Cell Catalysts. *J. Power Sources* **2009**, *192*, 57−62.
(36) Coloma, F.; Sepúlveda-Escribano, A.; Rodríguez-Roinoso, F. Heat-Treated Carbon Blacks as Supports for Platinum Catalysts. *J. Catal.* **1995**, *154*, 299−305.
(37) Granucci, G.; Persico, M. Benzene-O_2 Interaction Potential from Ab Initio Calculations. *Chem. Phys. Lett.* **1993**, *205*, 331−336.
(38) Giannozzi, P.; Car, R.; Scoles, G. Oxygen Adsorption on Graphite and Nanotubes. *J. Chem. Phys.* **2003**, *118*, 1003−1006.
(39) Masuda, T.; Naohara, H.; Takakusagi, S.; Singh, P. R.; Uosaki, K. Formation and Structure of Perfluorosulfonated Ionomer Thin Film on a Graphite Surface. *Chem. Lett.* **2009**, *38*, 884−885.
(40) Jiang, P.; Ma, X.; Ning, J.; Song, C.; Chen, X.; Jia, J.-F.; Xue, Q.-K. Quantum Size Effect Directed Selective Self-Assembling of Cobalt Phthalocyanine on Pb(111) Thin Films. *J. Am. Chem. Soc.* **2008**, *130*, 7790−7791.
(41) Cox, J. D.; Wagman, D. D.; Medvedev, V. A. *Codata Key Values for Thermodynamics*; Hemisphere Publishing Corporation: New York, 1984.
(42) Campbell, C. T.; Sellers, J. R. V. The Entropies of Adsorbed Molecules. *J. Am. Chem. Soc.* **2012**, *134*, 18109−18115.
(43) Stolyarova, E.; Rim, K. T.; Ryu, S.; Maultzsch, J.; Kim, P.; Brus, L. E.; Heinz, T. F.; Hybertsen, M. S.; Flynn, G. W. High-Resolution Scanning Tunneling Microscopy Imaging of Mesoscopic Graphene Sheets on an Insulating Surface. *Proc. Natl. Acad. Sci. U. S. A.* **2007**, *104*, 9209−9212.
(44) Kling, J.; Vestergaard, J. S.; Dahl, A. B.; Stenger, N.; Booth, T. J.; Bøggild, P.; Larsen, R.; Wagner, J. B.; Hansen, T. W. Pattern Recognition Approach to Quantify the Atomic Structure of Graphene. *Carbon* **2014**, *74*, 363−366.
(45) Sakai, T.; Takenaka, H.; Torikai, E. Gas Diffusion in the Dried and Hydrated Nafions. *J. Electrochem. Soc.* **1986**, *133*, 88−92.
(46) Zhang, L.; Ma, C.; Mukerjee, S. Oxygen Permeation Studies on Alternative Proton Exchange Membranes Designed for Elevated Temperature Operation. *Electrochim. Acta* **2003**, *48*, 1845−1859.
(47) Ito, H.; Maeda, T.; Nakano, A.; Takenaka, H. Properties of Nafion Membranes under PEM Water Electrolysis Conditions. *Int. J. Hydrogen Energy* **2011**, *36*, 10527−10540.
(48) Schmidt-Rohr, K.; Chen, Q. Parallel Cylindrical Water Nanochannels in Nafion Fuel-Cell Membranes. *Nat. Mater.* **2008**, *7*, 75−83.
(49) Pasternak, R. A.; Christensen, M. V.; Heller, J. Diffusion and Permeation of Oxygen, Nitrogen, Carbon Dioxide, and Nitrogen Dioxide through Polytetrafluoroethylene. *Macromolecules* **1970**, *3*, 366−371.
(50) Artyushkova, K.; Pylypenko, S.; Dowlapalli, M.; Atanassov, P. Structure-to-Property Relationships in Fuel Cell Catalyst Supports: Correlation of Surface Chemistry and Morphology with Oxidation Resistance of Carbon Blacks. *J. Power Sources* **2012**, *214*, 303−313.
(51) Ohma, A.; Fushinobu, K.; Okazaki, K. Influence of Nafion® Film on Oxygen Reduction Reaction and Hydrogen Peroxide Formation on Pt Electrode for Proton Exchange Membrane Fuel Cell. *Electrochim. Acta* **2010**, *55*, 8829−8838.
(52) Kangasniemi, K. H.; Condit, D. A.; Jarvi, T. D. Characterization of Vulcan Electrochemically Oxidized under Simulated PEM Fuel Cell Conditions. *J. Electrochem. Soc.* **2004**, *151*, E125−E132.
(53) Kozub, B. R.; Compton, R. G. Voltammetric Studies of the Redox Mediator, Cobalt Phthalocyanine, with Regard to Its Claimed Electrocatalytic Properties. *Sens. Actuators, B* **2010**, *147*, 350−358.
(54) Jung, H.-Y.; Kim, J. W. Role of the Glass Transition Temperature of Nafion 117 Membrane in the Preparation of the Membrane Electrode Assembly in a Direct Methanol Fuel Cell (DMFC). *Int. J. Hydrogen Energy* **2012**, *37*, 12580−12585.
(55) Benitez, R.; Soler, J.; Daza, L. Novel Method for Preparation of PEMFC Electrodes by the Electrospray Technique. *J. Power Sources* **2005**, *151*, 108−113.
(56) Yazdanpour, M.; Esmaeilifar, A.; Rowshanzamir, S. Effects of Hot Pressing Conditions on the Performance of Nafion Membranes Coated by Ink-Jet Printing of Pt/MWCNTs Electrocatalyst for PEMFCs. *Int. J. Hydrogen Energy* **2012**, *37*, 11290−11298.
(57) Inaba, M.; Kinumoto, T.; Kiriake, M.; Umebayashi, R.; Tasaka, A.; Ogumi, Z. Gas Crossover and Membrane Degradation in Polymer Electrolyte Fuel Cells. *Electrochim. Acta* **2006**, *51*, 5746−5753.

DOI: 10.1021/acs.jpcc.6b09523
J. Phys. Chem. C 2016, 120, 28038−28048